

Article

Tripeptide-Catalyzed Asymmetric Aldol Reaction Between α -ketoesters and Acetone Under Acidic Cocatalyst-Free Conditions

Kazumasa Kon ¹, Hiromu Takai ², Yoshihito Kohari ^{3,*}  and Miki Murata ^{1,2,3}

¹ Graduate School of Manufacturing Engineering, Kitami Institute of Technology, 165 Koen-Cho, Kitami, Hokkaido 090-8507, Japan; d1871300025@std.kitami-it.ac.jp

² Graduate School of Materials Science and Engineering, Kitami Institute of Technology, 165 Koen-Cho, Kitami, Hokkaido 090-8507, Japan; m1852600130@std.kitami-it.ac.jp

³ School of Earth, Energy and Environmental Engineering, Faculty of Engineering, Kitami Institute of Technology, 165 Koen-Cho, Kitami, Hokkaido 090-8507, Japan; muratamk@mail.kitami-it.ac.jp

* Correspondence: kohari@mail.kitami-it.ac.jp; Tel.: +81-157-26-9432

Received: 17 April 2019; Accepted: 6 June 2019; Published: 9 June 2019



Abstract: Here, we report the tripeptide-catalyzed asymmetric aldol reaction between α -ketoesters and acetone under acidic cocatalysts-free conditions. H-Pro-Tle-Gly-OH **3g**-catalyzed reactions between α -ketoesters and acetone resulted in up to 95% yield and 88% ee. Analysis of the transition state using density functional theory (DFT) calculations revealed that the *tert*-butyl group in **3g** played an important role in enantioselectivity.

Keywords: organocatalyst; aldol reaction; peptide catalyst; α -ketoesters

1. Introduction

Optically active tertiary alcohols are partial structures present in various natural products and biologically active compounds [1–5]. Various synthetic methods for these compounds have been developed. Asymmetric nucleophile addition to functionalized ketones is one of the most useful synthetic methods, because highly functionalized optically active tertiary alcohols, which can undergo various transformations, can be obtained. For example, the direct asymmetric aldol reaction between α -ketoesters and acyclic ketones is a helpful asymmetric reaction, because it gives γ -keto- α -hydroxyesters, which can undergo various transformations [6–8]. Therefore, various asymmetric catalysts, such as bisprolinamide, primary amine, and diamine catalysts, have been developed for this reaction [9–17]. However, most catalysts require acidic cocatalysts for high enantioselectivity and high chemical yield. Thus, simpler catalytic systems that do not require acidic cocatalysts are needed. Nevertheless, the number of asymmetric catalysts that catalyze this reaction, under acidic cocatalyst-free conditions, is limited. Although Zhang et al. [18] reported a proline-catalyzed asymmetric aldol reaction between ethyl phenylglyoxylate and acetone under acidic cocatalyst-free conditions, this method was enantioselective to some degree [18]. To the best of our knowledge, for this reaction, an asymmetric catalyst displaying high enantioselectivity and chemical yield under acidic cocatalyst-free conditions has still not been reported.

Following the introduction of a proline-catalyzed asymmetric aldol reaction of aldehydes reported by List et al. [19], prolinamide catalysts for this reaction have been actively developed [20,21]. Synthetic peptides in prolinamide catalysts, are recognized as effective catalysts for the direct asymmetric aldol reaction using aldehydes as electrophiles [22–33]. However, peptide catalysts for the direct asymmetric aldol reaction using ketones as electrophiles are limited [29,33–36]. Previously, we developed tripeptide catalysts (Supplementary Materials) that catalyzed the direct asymmetric aldol reaction of isatins or

trifluoromethyl ketones with acetone (Figure 1a) [37,38]. These catalysts, under acidic cocatalyst-free conditions, displayed good enantioselectivity and kinetics in these reactions. Herein, we will report the direct asymmetric aldol reaction between α -ketoesters and acetone catalyzed by tripeptide under acidic cocatalyst-free conditions (Figure 1b).

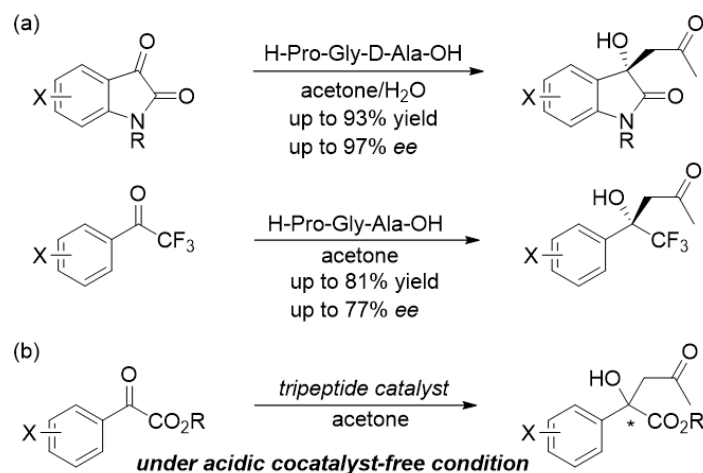


Figure 1. (a) Our previous works; (b) this work.

2. Results and Discussion

In this study, we investigated the effect of the catalyst structure on the rate and enantioselectivity of the reaction between methyl phenylglyoxylate (**1a**) and acetone (**2**) (Table 1, entries 1–9). H-Pro-Gly-Gly-OH **3a**-catalyzed reaction progressed to give the corresponding aldol adduct **4a** with 61% yield and 31% ee (Table 1, entry 1). To investigate the effect of introducing a methyl group to the C-terminal amino acid residue in **3a**, H-Pro-Gly-Ala-OH **3b**- and H-Pro-Gly-D-Ala-OH **3c**-catalyzed reactions were carried out (Table 1, entries 2 and 3). Both reactions displayed higher reaction rates than the **3a**-catalyzed reaction; however, enantioselectivities of both reactions were not improved, compared with that of the **3a**-catalyzed reaction. H-Pro-Ala-Gly-OH **3d**- and H-Pro-D-Ala-Gly-OH **3e**-catalyzed reactions introduced a methyl group to the amino acid residue adjacent to the proline residue in **3a**. The reaction between **1a** and **2** gave **4a** higher enantioselectivity than the **3a**-catalyzed reaction (Table 1, entries 4 and 5). The **3d**-catalyzed reaction displayed higher enantioselectivity than the **3e**-catalyzed one. However, the reaction catalyzed by H-Pro-Val-Gly-OH **3f** and H-Pro-Tle-Gly-OH **3g**, containing bulkier isopropyl and tertiary butyl groups instead of methyl groups, displayed higher enantioselectivities than the **3d**-catalyzed reaction (Table 1, entries 6–7). Above all, **3g**-catalyzed reactions showed the highest enantioselectivity and reaction rates than any of the other catalyzed reactions. From these investigations, it was discovered that bulky substitution in L-amino acid adjacent to proline residue played an important role in determining enantioselectivity. From the results, we decided that the most efficient catalyst for this reaction was **3g**, in terms of enantioselectivity and the reaction rate obtained.

To improve enantioselectivity, we optimized the reaction conditions for a **3g**-catalyzed reaction between **1a** and **2** (Table 1, entries 8–21). This reaction was carried out in various solvents (Table 1, entries 8–13). In THF and diethyl ether, the reaction displayed higher enantioselectivity than in any other solvent (Table 1, entries 12 and 13). The reaction in THF and diethyl ether at 0 °C produced **4a** with higher enantioselectivity than that at 20 °C. However, the reaction rate at 0 °C in diethyl ether was lower than that in THF at 0 °C. Therefore, we determined that the best solvent for this reaction was THF, in terms of enantioselectivity and reaction rate (Table 1, entries 14 and 15). The reaction in THF at –15 °C did not progress (Table 1, entry 16). The reaction in THF at 0 °C was also slow when the catalytic amount was reduced from 20 mol% to 10 mol% (Table 1, entry 17). The increase and decrease in the amounts of **2** and THF, respectively, caused a reduction in reaction rate (Table 1, entries

18–21). From all the reaction conditions tested, it was revealed that the optimum reaction was **3g** (20 mol%)-catalyzed reaction using **2** (100 eq.) in THF (1 mL) at 0 °C, because this reaction gave **4a** with 76% chemical yield and 88% ee under less acidic conditions (Table 1, entry 16).

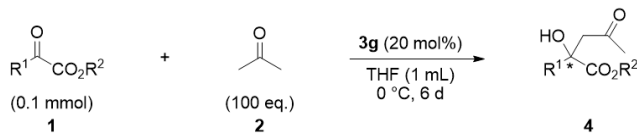
Table 1. Optimization of catalysts and reaction conditions.

Entry	Catalyst	Solvent	Yield (%) ^a	ee (%) ^b
1	H-Pro-Gly-Gly-OH 3a	neat	61	31
2	H-Pro-Gly-Ala-OH 3b	neat	81	30
3	H-Pro-Gly-D-Ala-OH 3c	neat	70	26
4	H-Pro-Ala-Gly-OH 3d	neat	50	38
5	H-Pro-D-Ala-Gly-OH 3e	neat	49	34
6	H-Pro-Val-Gly-OH 3f	neat	49	50
7	H-Pro-Ile-Gly-OH 3g	neat	90	65
8	3g	MeOH	40	30
9	3g	MeCN	62	54
10	3g	CHCl ₃	81	68
11	3g	PhMe	44	70
12	3g	THF	82	79
13	3g	Et ₂ O	74	82
14 ^c	3g	THF	76	88
15 ^c	3g	Et ₂ O	45	88
16 ^d	3g	THF	—	—
17 ^{c,e}	3g	THF	39	89
18 ^{c,f}	3g	THF	56	87
19 ^{c,g}	3g	THF	57	89
20 ^{c,h}	3g	THF	34	89
21 ^{c,i}	3g	THF	56	83

^a Isolated yield after preparative thin layer chromatography. ^b Determined by HPLC. Absolute configuration of **4a** was determined by comparing optical rotation between **4a** and previous report [14]. ^c Reaction was carried out at 0 °C. ^d Reaction was carried out at −15 °C. ^e **3g** (10 mol%) was used. ^f **2** (150 eq.) was used. ^g **2** (50 eq.) was used. ^h Reaction was carried out in THF (2 mL). ⁱ Reaction was carried out in THF (0.5 mL).

We also investigated the reaction between various α -ketoesters **1a–1h** and **2** under optimized conditions (Table 2). To reveal the effect of ester substituents, reactions of **1a–1c** having various ester groups were carried out (Table 2, entries 1–3). In reactions using **1a–1c** as substrates with alkyl esters, the bulkier the alkyls esters were, the slower the reactions progressed. The substrates **1a–1c** generated the corresponding aldol adducts **4a–4c** with good enantioselectivities. To estimate the contribution of the methoxycarbonyl group of **1a**, the reaction between acetophenone and acetone was carried out. This reaction was not progressed. To investigate the effect of substituents on phenyl groups, reactions of 4-substituted α -ketoesters **1d–1g** were carried out (Table 2, entries 4–7). Reactions of 4-Cl **1d** and 4-CF₃ **1e** were faster than that of **1a**, and especially that of **1e**, which was completed after three days. However, enantioselectivities of reactions **1d** and **1e** were lower than that of the reaction of **1a** (Table 2, entries 4 and 5, respectively). In the reactions of 4-Me **1f** and 4-MeO **1g**, the reaction rates and enantioselectivities were also lower than that of the reaction of **1a** (Table 2, entries 6 and 7, respectively). The reactions of methyl pyruvate (**1h**) and methyl trimethylpyruvate as aliphatic α -ketoesters were investigated. The reaction between **1h** and **2** gave corresponding aldol adduct **4h**, with good chemical yield and medium enantioselectivity (Table 2, entry 8). Additionally, the reaction of more bulky genusmethyl trimethylpyruvate (R¹ = *t*Bu) with **2** did not give corresponding aldol adduct. Cyclohexanone, 2-butanone, and acetophenone were applied as nucleophiles. These nucleophiles were not reacted.

Table 2. Substrate scope.



Entry	R ¹	R ²	1	4	Yield (%) ^a	ee (%) ^b
1	Ph	Me	1a	4a	76	88(R) ^c
2	Ph	Et	1b	4b	63	82
3	Ph	<i>i</i> Pr	1c	4c	33	86
4	4-CIPh	Me	1d	4d	84	75
5 ^d	4-CF ₃ Ph	Me	1e	4e	95	50
6	4-MePh	Me	1f	4f	25	75
7	4-MeOPh	Me	1g	4g	10	65
8	Me	Me	1h	4h	92	39

^a Isolated yield after preparative thin layer chromatography. ^b Determined by HPLC. ^c Absolute configuration of **4a** was determined by comparing optical rotation between **4a** and previous report [14]. ^d Reaction was demonstrated for **3d**.

It was assumed that the catalytic cycle of this reaction was similar to that of the proline-catalyzed asymmetric aldol reaction (Figure 2a) [9]. Therefore, **2** was activated by enamine formation by reacting with the amino group of **3g**. The C–C bond was then formed by nucleophilic addition to the **1** of enamine as a nucleophile to generate the iminium cation. Finally, the aldol adduct was produced by the hydrolysis of the iminium cation. In this reaction, the absolute configuration of the aldol adduct **4** was determined at the C–C bond formation step.

To understand the effect of *tert*-leucine residue in H-Pro-Tle-Gly-OH **3g** on enantioselectivity, origins of enantioselectivity of **3g** and H-Pro-Gly-Gly-OH **3a** were investigated. Specifically, transition states of the stereo-determining C–C bond forming step of **3g**- and **3a**-catalyzed reactions between **1a** and **2** were investigated via density functional theory (DFT) calculations (Figures 2b and 3) [39,40].

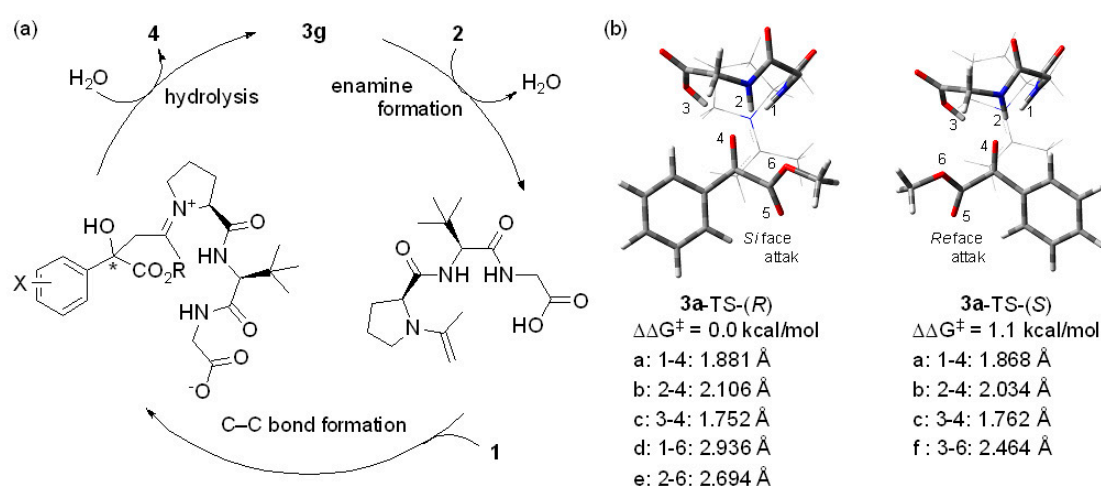


Figure 2. (a) A plausible catalytic cycle; (b) transition states of C–C bond forming step of **3a**-catalyzed reaction between **1a** and **2**. All calculations were carried out via CPCM(acetone)/B3LYP/6-31G(d',p')//B3LYP/6-31G(d',p') level of theory.

Investigation of transition states of the stereo-determining C–C bond forming step of **3a**-catalyzed reactions between **1a** and **2** via DFT calculations revealed that the major (*R*)-aldol adduct was produced through **3a-TS-(R)**, and the minor (*S*)-aldol adduct was produced through **3a-TS-(S)** in the **3a**-catalyzed reaction (Figure 2b). Like the experimental result where (*R*)-aldol adduct was preferentially obtained

(Table 1, entry 1), **3a-TS-(R)** was the more stable transition state. To understand the origin of enantioselectivity of **3a**, we focused on hydrogen bonds in transition states of the stereo-determining C–C bond forming step. Hydrogen bonds a, b, and c were formed in both transition states. However, hydrogen bonds d and e were present in only **3a-TS-(R)**, and hydrogen bond f was present in only **3a-TS-(S)**. Namely, **3a-TS-(R)** had more hydrogen bonds than **3a-TS-(S)**. This was the reason why **3a-TS-(R)** was the more stable transition state. The investigation of transition states of the C–C bond forming step of the **3g**-catalyzed reaction via DFT calculation found four transition states, such as **3g-TS-(R)-1**, **3g-TS-(R)-2**, **3g-TS-(S)-1**, and **3g-TS-(S)-2** (Figure 3). When this **3g**-catalyzed reaction passed through **3g-TS-(R)-1** and **3g-TS-(R)-2**, the major (*R*)-aldol adduct was obtained. Similarly, when this **3g**-catalyzed reaction passed through **3g-TS-(S)-1** and **3g-TS-(S)-2**, the minor (*S*)-aldol adduct was obtained. Focusing on conformations of these transition states, **3g** in **3g-TS-(R)-1** and **3g-TS-(S)-1** had a similar conformation to **3a** in the transition state of the C–C bond forming step of the **3a**-catalyzed reaction. However, the presence of **3g** in these transition states introduced steric repulsion between the ^{*t*}Bu of *tert*-leucine residue and the carbonyl group of proline residue, causing destabilization of these transition states. In contrast, this steric repulsion was mitigated in **3g-TS-(R)-2** and **3g-TS-(S)-2**, due to the change in conformation influenced by the ^{*t*}Bu group. Due to this change of steric environment in these transition states, **3g-TS-(R)-2** and **3g-TS-(S)-2** were more stable than **3g-TS-(R)-1** and **3g-TS-(S)-1**. For that reason, it was concluded that (*S*)- and (*R*)-aldol adducts were formed through **3g-TS-(S)-2** and **3g-TS-(R)-2** in the **3g**-catalyzed reaction, respectively.

Finally, **3g-TS-(R)-2** and **3g-TS-(S)-2** were analyzed and a comparison of their Gibbs free energy revealed that **3g-TS-(R)-2** was 2.2 kcal/mol more stable than **3g-TS-(S)-2**. This difference in Gibbs free energy was larger than that between **3a-TS-(R)** and **3a-TS-(S)**. Moreover, DFT calculations reproduced the experimental results such that **3g** displayed higher enantioselectivity than **3a**, mainly because of the difference in stabilization caused by hydrogen bonds. In both **3g-TS-(R)-2** and **3g-TS-(S)-2**, multiple hydrogen bonds a, b, and c formed. Hydrogen bonds g and h formed only in **3g-TS-(R)-2**. The conformational change of **3g** by the introduction of ^{*t*}Bu group to **3a** created a larger difference in the number of hydrogen bonds formed between **3g-TS-(R)-2** and **3g-TS-(S)-2** than that between **3a-TS-(R)** and **3a-TS-(S)**. Hence, difference of stabilization by hydrogen bonds between **3g-TS-(R)-2** and **3g-TS-(S)-2** was larger than that between **3a-TS-(R)** and **3a-TS-(S)**. From the above results, we concluded that the control of **3g** conformation by ^{*t*}Bu groups played an important role in the production of enantioselectivity.

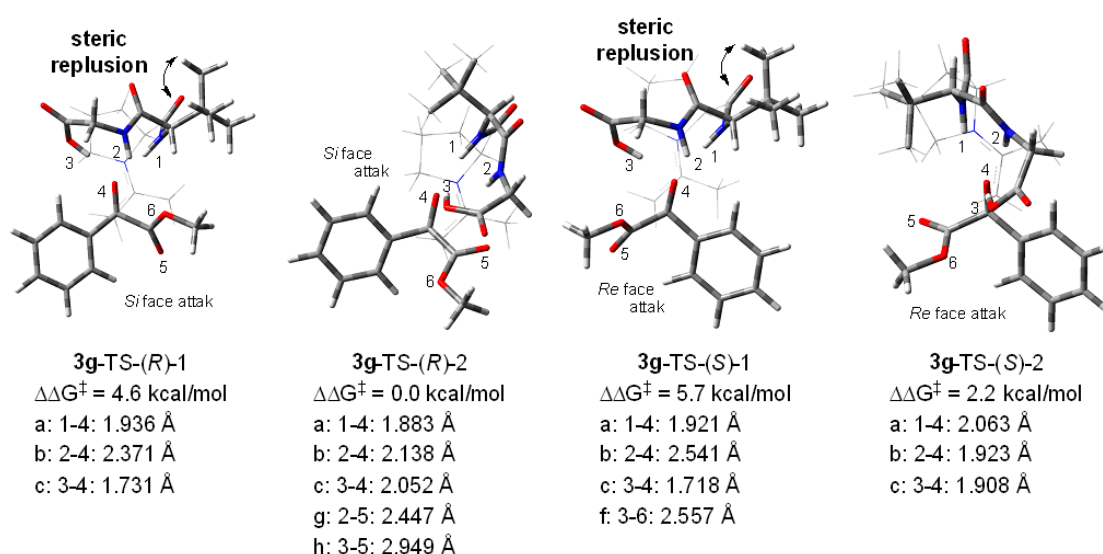


Figure 3. Transition states of C–C bond forming step of **3g**-catalyzed reaction between **1a** and **2**. All calculations were carried out via CPCM(acetone)/B3LYP/6-31G(d',p')// B3LYP/6-31G(d',p') level of theory.

3. Materials and Methods

3.1. General Methods

Column chromatography was carried out on a column packed with spherical silica gel 60N of neutral size, 40–50 μm . Thin layer chromatography was prepared using PLC Silica gel (60 F₂₅₄, 1 mm, Merck). NMR spectra were recorded on a JEOL JNM-ECA600 spectrometer (¹H, 600 MHz; ¹³C, 150 MHz). Chemical shifts of ¹H NMR and ¹³C NMR signals, reported as δ ppm, were referenced to an internal standard SiMe₄ or sodium 3-(trimethylsilyl)-1-propanesulfonate. HRMS were obtained at an ionization potential of 70 eV with a JEOL JMS-T100GCV spectrometer. Melting points were measured on an AS ONE ATM-01 melting-point apparatus. Optical rotations were measured by a JASCO P-1010 Polarimeter. HPLC analysis was performed with a Daicel Chiralpak AD-H column (25 cm \times 4.6 mm \times 5 μm) and Chiralpak OD-H column (25 cm \times 4.6 mm \times 5 μm). All reagents and solvents were purchased from commercial sources and used without purification. Compounds **1a–1g** were synthesized by the previously reported method [41,42]. Tripeptide catalysts were synthesized by the literature methods [37,38].

3.2. General Procedure for the Asymmetric Aldol Reaction between α -Ketoesters and Acetone

A mixture of H-Pro-Tle-Gly-OH **3g** (20 μmol , 5.7 mg), acetone (10 mmol, 0.74 mL), and THF (1.0 mL) was stirred at 0 $^{\circ}\text{C}$ for 10 min. To the resulting mixture, α -ketoester (0.1 mmol) was added. The mixture was stirred at 0 $^{\circ}\text{C}$ for six days and then filtered to remove the catalyst. The resulting mixture was concentrated under reduced pressure. Preparative thin layer chromatography on silica gel using hexane/ethyl acetate as the eluent gave the aldol adduct. The enantiomeric excess of aldol adduct was determined by chiral HPLC.

4. Conclusions

We have developed a direct asymmetric aldol reaction between α -ketoesters and acetone, catalyzed by a tripeptide under acidic cocatalyst-free conditions. The **3g**-catalyzed reaction gave various aldol adducts with up to 95% yield and 88% ee. Investigation of the transition state via the C–C bond forming step by DFT calculations has revealed the role of the ^tBu group in **3g** in determining enantioselectivity.

Supplementary Materials: The following are available online at <http://www.mdpi.com/2073-4344/9/6/514/s1>, 1. General; 2. Materials; 3. Preparation of the tripeptide catalysts; 4. General procedure for tripeptide-catalyzed asymmetric aldol reaction; 5. Computational Details; 6. Reference; 7. Copy of NMR spectra; 8. Copy of HPLC spectra; 9. Geometries and Cartesian Coordinates. Figure S1: Synthesis of tripeptide catalysts.

Author Contributions: K.K. and M.M. designed the experiments. K.K. and Y.K. wrote the paper. K.K. and H.T. performed the experiments. All authors read and approved the final manuscript.

Funding: This research received no external funding.

Conflicts of Interest: The authors declare no conflict of interest.

References

1. Trost, B.M.; Dirat, O.; Gunzner, J.L. Callipeltoside A: Assignment of Absolute and Relative Configuration by Total Synthesis. *Angew. Chem. Int. Ed.* **2002**, *41*, 841–843. [[CrossRef](#)]
2. Maki, K.; Motoki, R.; Fujii, K.; Kanai, M.; Kobayashi, T.; Tamura, S.; Shibasaki, M. Catalyst-Controlled Asymmetric Synthesis of Fostriecin and 8-*epi*-Fostriecin. *J. Am. Chem. Soc.* **2005**, *127*, 17111–17117. [[CrossRef](#)] [[PubMed](#)]
3. Lei, X.; Porco, J.A. Total Synthesis of the Diazobenzofluorene Antibiotic (–)-Kinamycin C¹. *J. Am. Chem. Soc.* **2006**, *128*, 14790–14791. [[CrossRef](#)] [[PubMed](#)]
4. Nicolaou, K.C.; Li, H.; Nold, A.L.; Pappo, D.; Lenzen, A. Total Synthesis of Kinamycins C, F, and J. *J. Am. Chem. Soc.* **2007**, *129*, 10356–10357. [[CrossRef](#)]
5. Carpenter, J.; Northrup, A.B.; Chung, D.; Wiener, J.J.M.; Kim, S.-G.; MacMillan, D.W.C. Total Synthesis and Structural Revision of Callipeltoside C. *Angew. Chem. Int. Ed.* **2008**, *47*, 3568–3572. [[CrossRef](#)] [[PubMed](#)]

6. Tokuda, O.; Kano, T.; Gao, W.-G.; Ikemoto, T.; Maruoka, K. A Practical Synthesis of (S)-2-Cyclohexyl-2-phenylglycolic Acid via Organocatalytic Asymmetric Construction of a Tetrasubstituted Carbon Center. *Org. Lett.* **2005**, *7*, 5103–5105. [[CrossRef](#)] [[PubMed](#)]
7. Xu, X.-Y.; Tang, Z.; Wang, Y.-Z.; Luo, S.-W.; Cun, L.-F.; Gong, L.-Z. Asymmetric Organocatalytic Direct Aldol Reactions of Ketones with α -Keto Acids and Their Application to the Synthesis of 2-Hydroxy- γ -butyrolactones. *J. Org. Chem.* **2007**, *72*, 9905–9913. [[CrossRef](#)]
8. Zheng, C.; Wu, Y.; Wang, X.; Zhao, G. Highly Enantioselective Organocatalyzed Construction of Quaternary Carbon Centers *via* Cross-Aldol Reaction of Ketones in Water. *Adv. Synth. Catal.* **2008**, *350*, 2690–2694. [[CrossRef](#)]
9. Wang, F.; Xiong, Y.; Liu, X.; Feng, X. Asymmetric Direct Aldol Reaction of α -Keto Esters and Acetone Catalyzed by Bifunctional Organocatalysts. *Adv. Synth. Catal.* **2007**, *349*, 2665–2668. [[CrossRef](#)]
10. Liu, J.; Yang, Z.; Wang, Z.; Wang, F.; Chen, X.; Liu, X.; Feng, X.; Su, Z.; Hu, C. Asymmetric Direct Aldol Reaction of Functionalized Ketones Catalyzed by Amine Organocatalysts Based on Bispidine. *J. Am. Chem. Soc.* **2008**, *130*, 5654–5655. [[CrossRef](#)]
11. Liu, Q.-Z.; Wang, X.-L.; Luo, S.-W.; Zheng, B.-L.; Qiu, D.-B. Facile Preparation of Optically Pure Diamines and Their Applications in Asymmetric Aldol Reactions. *Tetrahedron Lett.* **2008**, *49*, 7434–7437. [[CrossRef](#)]
12. Raj, M.; Parashari, G.S.; Singh, V.K. Highly Enantioselective Organocatalytic *syn*- and *anti*-Aldol Reactions in Aqueous Medium. *Adv. Synth. Catal.* **2009**, *351*, 1284–1288. [[CrossRef](#)]
13. Jiang, Z.; Lu, Y. Direct asymmetric aldol reaction of acetone with α -ketoesters catalyzed by primary–tertiary diamine organocatalysts. *Tetrahedron Lett.* **2010**, *51*, 1884–1886. [[CrossRef](#)]
14. Zhu, X.; Liu, A.; Fang, L.; Li, W.; Zhu, C.; Cheng, Y. In Situ Formed Bifunctional Primary Amine–Imine Catalyst for Asymmetric Aldol Reactions of α -Keto Esters. *Chem. Eur. J.* **2011**, *17*, 8281–8284. [[CrossRef](#)] [[PubMed](#)]
15. Viózz, S.F.; Bañón-Caballero, A.; Guillena, G.; Nájera, C.; Gómez-Bengoa, E. Enantioselective Direct Aldol Reaction of α -keto esters Catalyzed by (*S*_A)-binam-D-prolinamide under Quasi Solvent-Free Conditions. *Org. Biomol. Chem.* **2012**, *10*, 4029–4035.
16. Lisnyak, V.G.; Kucherenko, A.S.; Valeev, E.F.; Zlotin, S.G. (1,2-Diaminoethane-1,2-diyl)bis(*N*-methylpyridinium) Salts as a Prospective Platform for Designing Recyclable Prolinamide-Based Organocatalysts. *J. Org. Chem.* **2015**, *80*, 9570–9577. [[CrossRef](#)] [[PubMed](#)]
17. Kochetkov, S.V.; Kucherenko, A.S.; Zlotin, S.G. Asymmetric Aldol Reactions in Ketone/ketone Systems Catalyzed by Ionic Liquid-Supported C₂-symmetrical Organocatalyst. *Mendeleev Commun.* **2015**, *25*, 168–170. [[CrossRef](#)]
18. Wang, Y.-J.; Shen, Z.-X.; Li, B.; Zhang, Y.-W. Proline Catalyzed Asymmetric Aldol Reaction between Methyl Ketones and α -Ketoesters. *Chin. J. Chem.* **2006**, *24*, 1196–1199. [[CrossRef](#)]
19. List, B.; Lerner, A.R.; Barbas, C.F. Proline-Catalyzed Direct Asymmetric Aldol Reactions. *J. Am. Chem. Soc.* **2000**, *122*, 2395–2396. [[CrossRef](#)]
20. Bisai, V.; Bisai, A.; Singh, V.K. Enantioselective Organocatalytic Aldol Reaction Using Small Organic Molecules. *Tetrahedron* **2012**, *68*, 4541–4580. [[CrossRef](#)]
21. Heravi, M.M.; Zadsirjan, V.; Dehghani, M.; Hosseintash, N. Current Applications of Organocatalysts in Asymmetric Aldol Reactions: An Update. *Tetrahedron: Asymmetry* **2017**, *28*, 587–707. [[CrossRef](#)]
22. Shi, L.-X.; Sun, Q.; Ge, Z.-M.; Zhu, Y.-Q.; Cheng, T.-M.; Li, R.-T. Dipeptide-Catalyzed Direct Asymmetric Aldol Reaction. *Synlett* **2004**, *12*, 2215–2217. [[CrossRef](#)]
23. Krattiger, P.; Kovásy, R.; Revell, J.D.; Wennemers, H. Using Catalyst–Substrate Coimmobilization for the Discovery of Catalysts for Asymmetric Aldol Reactions in Split-and-Mix Libraries. *QSAR Comb. Sci.* **2005**, *24*, 1158–1163. [[CrossRef](#)]
24. Krattiger, P.; Kovásy, R.; Revell, J.D.; Ivan, S.; Wennemers, H. Increased Structural Complexity Leads to Higher Activity: Peptides as Efficient and Versatile Catalysts for Asymmetric Aldol Reactions. *Org. Lett.* **2005**, *7*, 1101–1103. [[CrossRef](#)] [[PubMed](#)]
25. Revell, J.D.; Gantenbein, D.; Krattiger, P.; Wennemers, H. Solid-Supported and Pegylated H–Pro–Pro–Asp–NHR as Catalysts for Asymmetric Aldol Reactions. *Biopolymers (Pept. Sci.)*. **2006**, *84*, 105–113. [[CrossRef](#)] [[PubMed](#)]
26. Dodda, R.; Zhao, C.-G. Organocatalytic Enantioselective Synthesis of Secondary α -Hydroxycarboxylates. *Synlett* **2007**, *10*, 1605–1609. [[CrossRef](#)]

27. D'Elia, V.; Zwicknagl, H.; Reiser, O. Short α/β -Peptides as Catalysts for Intra- and Intermolecular Aldol Reactions. *J. Org. Chem.* **2008**, *73*, 3262–3265. [[CrossRef](#)] [[PubMed](#)]
28. Wu, F.-C.; Da, C.-S.; Du, Z.-X.; Guo, Q.-P.; Li, W.-P.; Yi, L.; Jia, Y.-N.; Ma, X. N-Primary-Amine-Terminal β -Turn Tetrapeptides as Organocatalysts for Highly Enantioselective Aldol Reaction. *J. Org. Chem.* **2009**, *74*, 4812–4818. [[CrossRef](#)] [[PubMed](#)]
29. Pearson, A.J.; Panda, S. N-Prolinylanthranilamide Pseudopeptides as Bifunctional Organocatalysts for Asymmetric Aldol Reactions. *Org. Lett.* **2011**, *13*, 5548–5551. [[CrossRef](#)] [[PubMed](#)]
30. Barrulas, P.; Benaglia, M.; Burke, A.J. Synthesis of Novel Cinchona-Amino Acid Hybrid Organocatalysts for Asymmetric Catalysis. *Tetrahedron: Asymmetry* **2014**, *25*, 923–935. [[CrossRef](#)]
31. Szöllösi, G.; Csámpai, A.; Somlai, C.; Fekete, M.; Bartók, M. Unusual enantioselectivities in heterogeneous organocatalyzed reactions: Reversal of direction using proline di- versus tri-peptides in the aldol addition. *J. Mol. Catal. A: Chem.* **2014**, *382*, 86–92. [[CrossRef](#)]
32. Milbeo, P.; Maurent, K.; Moulat, L.; Lebrun, A.; Didierjean, C.; Aubert, E.; Martinez, J.; Calmès, M. N-Pyrrolidine-Based α/β -peptides Incorporating ABOC, A Constrained Bicyclic β -Amino Acid, for Asymmetric Aldol Reaction Catalysis. *Tetrahedron* **2016**, *72*, 1706–1715. [[CrossRef](#)]
33. Vlasserou, I.; Sfetsa, M.; Gerokonstantis, D.-T.; Kokotos, C.G.; Moutevelis-Minakakis, P. Combining Prolinamides with 2-pyrrolidinone: Novel Organocatalysts for The Asymmetric Aldol Reaction. *Tetrahedron* **2018**, *74*, 2338–2349. [[CrossRef](#)]
34. Luppi, G.; Cozzi, P.G.; Monari, M.; Kaptein, B.; Broxterman, Q.B.; Tomasini, C. Dipeptide-Catalyzed Asymmetric Aldol Condensation of Acetone with (N-Alkylated) Isatins. *J. Org. Chem.* **2005**, *70*, 7418–7421. [[CrossRef](#)]
35. Córdova, A.; Zou, W.; Dziejczak, P.; Ibrahim, I.; Reyes, E.; Xu, Y. Direct Asymmetric Intermolecular Aldol Reactions Catalyzed by Amino Acids and Small Peptides. *Chem. Eur. J.* **2006**, *12*, 5383–5397. [[CrossRef](#)]
36. Luppi, G.; Monari, M.; Corrêa, R.J.; Violante, F.A.; Pinto, A.C.; Kaptein, B.; Broxterman, Q.B.; Garden, S.J.; Tomasini, C. The First Total Synthesis of (R)-convolutamydine A. *Tetrahedron* **2006**, *62*, 12017–12024. [[CrossRef](#)]
37. Kon, K.; Kohari, Y.; Murata, M. Unnatural Tripeptide as Highly Enantioselective Organocatalyst for Asymmetric Aldol Reaction of Isatins. *Tetrahedron Lett.* **2019**, *60*, 415–418. [[CrossRef](#)]
38. Kon, K.; Kohari, Y.; Murata, M. Tripeptide-Catalyzed Asymmetric Aldol Reaction of Trifluoromethylated Aromatic Ketones with Acetone. *Heterocycles* **2019**, *99*, 841–847.
39. Frisch, M.J.; Trucks, G.W.; Schlegel, H.B.; Scuseria, G.E.; Robb, M.A.; Cheeseman, J.R.; Montgomery, J.A., Jr.; Vreven, T.; Kudin, K.N.; Burant, J.C.; et al. Gaussian 03, Revision C.02. Gaussian, Inc.: Wallingford, CT, USA, 2004. Available online: <https://gaussian.com/g03citation/> (accessed on 8 June 2019).
40. Frisch, M.J.; Trucks, G.W.; Schlegel, H.B.; Scuseria, G.E.; Robb, M.A.; Cheeseman, J.R.; Scalmani, G.; Barone, V.; Mennucci, B.; Petersson, G.A.; et al. Gaussian 09, Revision E.01. Gaussian, Inc.: Wallingford, CT, USA, 2009. Available online: <https://gaussian.com/g09citation/> (accessed on 8 June 2019).
41. Szőri, K.; Balázsik, K.; Felföldi, K.; Bartók, M. Study of Enantioselective Hydrogenation of Bulky Esters of Phenylglyoxylic Acid on Pt-CD and Pt- β -ICN Chiral Catalysts: Steric Effect of Ester Groups and Inversion of Enantioselectivity. *J. Catal.* **2006**, *241*, 149–154. [[CrossRef](#)]
42. Creary, X. Reaction of Organometallic Reagents with Ethyl Trifluoroacetate and Diethyl Oxalate. Formation of Trifluoromethyl Ketones and α -Keto Esters via Stable Tetrahedral Adducts. *J. Org. Chem.* **1987**, *52*, 5026–5030. [[CrossRef](#)]

